Steel Innovations Conference 2013
Christchurch, New Zealand
21-22 February 2013

CHARACTERISATION OF VELOCITY EFFECTS, CORROSION COATINGS AND SHIM MATERIALS ON INITIAL PERFORMANCE AND DEGRADATION OF SLIDING STEEL FRICTION CONNECTIONS

R. Causse[1], G.W. Rodgers[2], J.G. Chase[3], J. Chanchi[4], G.A. MacRae[5], and C. Clifton[6]

ABSTRACT

It has become increasingly necessary to develop systems to decrease the impact of earthquakes, to protect people and to mitigate the resulting structural and economic damage. The Asymmetrical Friction Connection (AFC) or Sliding Hinge Joint (SHJ) has been intensively tested. It efficiently dissipates energy with almost no damage. However, its nonlinear mechanics have not fully been characterised.

In this research, the AFC mechanism is modelled and parameterised using non-linear modelling. Menegotto-Pinto models of device behaviour including added velocity dependence are validated against a series of experimental tests. These SHJs are modelled for several shim (friction sliding surface) materials, as well as with and without corrosion resistant coatings.

The non-linear models developed accurately capture the experimentally observed nonlinear mechanics. The impact of shim material and corrosion coating on resistive force and velocity dependence are quantified. In particular, corrosion coatings create negative velocity dependence from a positive dependence without the coating. The overall modelling approach is suitable for use in a wide range of similar dynamic systems. Thus, the results also validate the overall modelling methods and the approach presented.

Introduction

The large earthquakes that have struck Christchurch have highlighted the potential for death, damage and downtime due to large seismic events. Earthquakes can produce significant damage in structures, especially in the beam/column connections that define the overall architecture and load carrying capacity. In particular, the displacement caused by a large earthquake dissipates significant energy, but may degrade the structural integrity and render a structure unusable. It costs time and significant economic resource to rebuild a city (10-20 years) after a major earthquake, and even more to regain lost prosperity back to the region. Consequently, many researchers are trying to find mechanisms to increase structural life and significantly reduce economic cost by decreasing damage due to seismic events. The development of damage-free methods of structural response and energy dissipation are at the forefront of a significant amount of research. This work focuses on one type of damage free connection, the Sliding Hinge joint (SHJ), which dissipates energy at beam-column connections through a controlled friction mechanism.

The objective of the work is the analysis and modelling of a large series of experimental results performed at the University of Canterbury. Using a well known, fundamental elasto-plastic model, a nonlinear mechanics model is derived to describe the general behaviour. Parameter values specific to friction materials and corrosion coatings are identified to create a general model capable of capturing a wide range of SHJ connection mechanics.

[1] Internship student, Dept. of Mechanical Engineering, University of Canterbury, Christchurch 8140, New Zealand
[2] Lecturer, Dept. of Mechanical Engineering, University of Canterbury, Christchurch 8140, New Zealand
[3] Professor, Dept. of Mechanical Engineering, University of Canterbury, Christchurch 8140, New Zealand
[4] PhD Student, Dept. of Civil Engineering, University of Canterbury, Christchurch 8140, New Zealand
[5] Associate Professor, Dept. of Civil Engineering, University of Canterbury, Christchurch 8140, New Zealand
[6] Associate Professor, Dept. of Civil Engineering, University of Auckland, New Zealand

Sliding Hinge Joint Mechanism

The SHJ, presented below in Figure 1, is a combination of plates of different materials, which are assembled to dissipate seismic energy. This friction connection has been developed as a low-cost, efficient means to protect structures from earthquakes. The manufacturing process of SHJs is straightforward, and the friction mechanism enables the repeatable dissipation of seismic energy to keep the structure in the elastic domain without damaging the overall connection. The end result is minimal damage, where typical rigid fixed connections may have yielded to dissipate energy, resulting in significant damage and economic loss. Ultimately, the SHJ provides an alternate energy dissipation mechanism to the yielding of steel frame elements and the formation of plastic hinge joint. The SHJ (also called Asymmetrical Friction Connections or AFC) have been extensively tested (Golondrino et al (2012)).

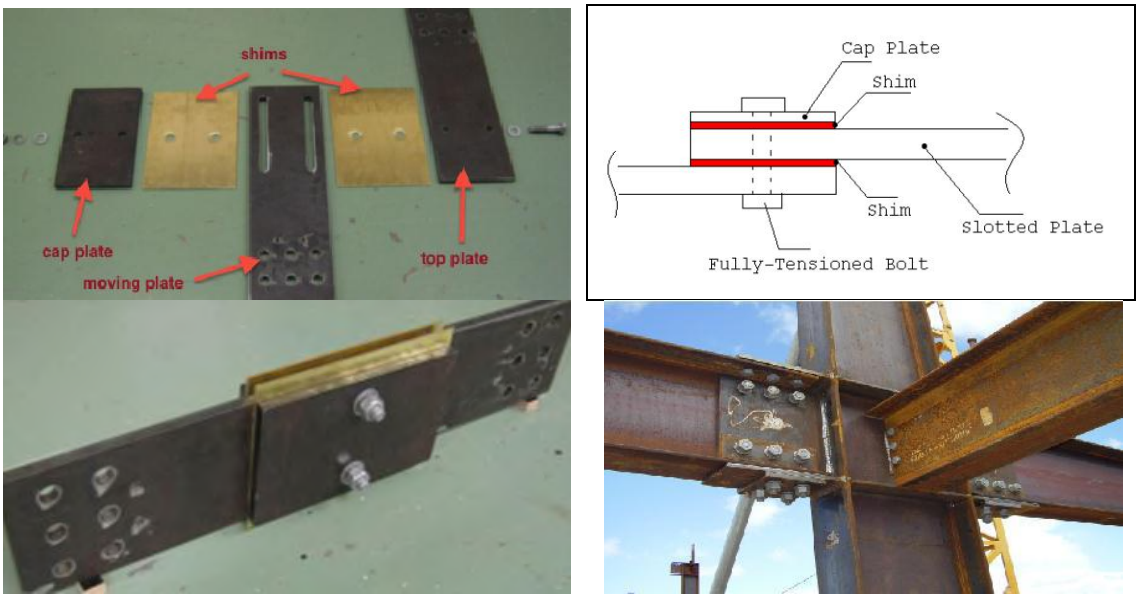

Figure 1. Sliding Hinge Joint mechanism (Golondrino et al (2012)); disassembled device (top left), two assembled views (top right and bottom left) and column/beam connection using the design approach (bottom right)

The SHJ consists of three different plates (made of steel) and two shims held together with bolts, as shown in Figure 1. The two long plates are called the moving plate and the top plate. They are drilled, enabling them to be fixed on both sides of the beams and columns to which they connect. The slots within the moving plates enable the mechanism to translate when the beam and the column move. Between those three plates, shims are placed to provide friction surfaces.

The movement of the moving plate generates friction forces in the interface between the moving plate and the shims, which propagates into the extremity of the mechanism (top and cap plates). Static and kinetic friction forces are dependent on the shim materials used and construction quality. Bolt tension is a particularly sensitive parameter in determining the resulting normal force on the shim and thus the actual device dissipation force.

Applications of the Sliding Hinge Joint

Figure 2 presents different possibilities for building structures with AFC connections on single or concentrically braced frames. For single braced frames, one of the possibilities is to place the AFC at the end of the frame (Figure 2-1). It offers the advantage of being easily replaceable when damage occurs. The second alternative is to cut off the frame and fix the resulting pinned connection with the AFC (Figure 2-2). For concentrically braced frames, the AFC can be placed in two basic configurations. The AFC is directly attached to the beam bottom flange, but the two configurations differ in the arrangement of the AFC. The first solution (Figure 2-3) places the AFC in a vertical arrangement. The second configuration is a near horizontal arrangement in Figure 2-4. (In fact the sliding is on a shallow arc). The beam bottom flange is slotted and braces can be welded or bolted to a vertical plate welded to a horizontal plate located below the beam; two cap plates are required to be placed above the beam bottom flange.

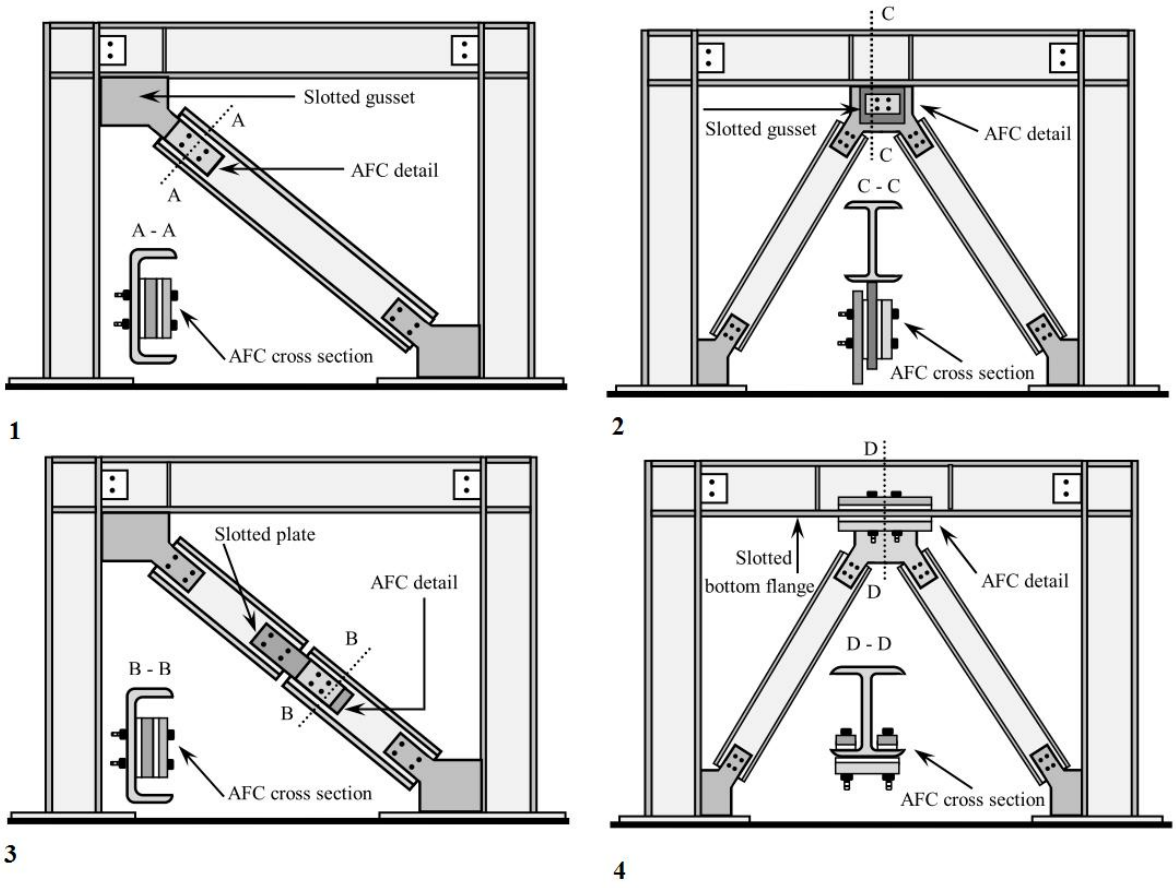

Figure 2. Applications of AFC on single and concentrically braced frames (Golondrino et al (2012)), single braced frames (top right and left) and concentrically frames (bottom right and left)

The SHJ have the following properties (Golondrino et al (2012), MacRae (2008) Clifton et al (2004)):

- Long slots in the moving plate increase the displacement capacity.
- The bolts (amount of tensioning) control the friction force.
- Damage (if any) remains in the SHJ only and is not transmitted to the frames.
- The cost is low due to simple construction

The SHJ is intended for structures that may be subject to high excitation. Connections for steel braced frames have been proposed by Clifton (2005), Clifton et al. (2004) and Clifton et al (2007). Different studies have shown a range of possible mechanical behaviours (Golondrino et al (2012), Clifton et al (2004) and Khoo et al (2012)). Nevertheless, other methods also exist to dissipate high energy levels in structural connections (Rodgers et al (2007), Rodgers et al (2008) and Golondrino et al (2012)).

Methods

Sliding Hinge Joint Test Input Profiles

This research models SHJ connections using data from sinusoidal input experiments at several amplitudes, but constant peak velocity of 10mm.s-1. The input displacement corresponds to six consecutive regimes of different amplitude, varying from 6.25% to 100% of the total SHJ slot length of 220mm. The first five regimes are composed of three sinusoidal cycles and the last of 5 cycles, making a total of 20 cycles. Figure 3 and Table 1 show the input displacement details.

To assess degradation, each SHJ connection was subjected to two 20-cycles regimes. Time, displacement, and force are recorded for all tests. The displacement recorded includes both the overall test machine input motion and the direct displacement across the SHJ connection.

Table 1. Components of the displacement loading regime .

Component	Tested Stroke (%)	(mm)	Max. Velocity (mm/s)	Frequency (Hz)	Cycles (#)
1	6.25	±6	10	0.27	3
2	12.5	±12	10	0.13	3
3	25	±24	10	0.067	3
4	50	±48	10	0.034	3
5	75	±72	10	0.022	3
6	100	±95	10	0.017	6

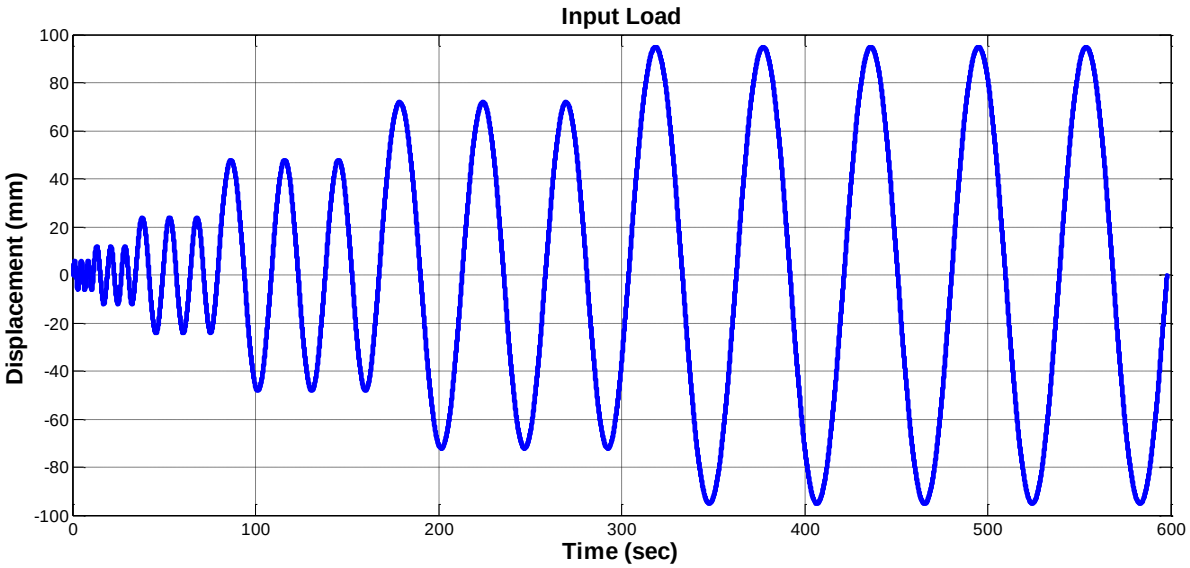

Figure 3. Loading Regime: Input displacement (mm) over time (s)

Sliding Hinge Joint Shim Materials

Six shim materials were tested to quantify the impact on friction force and the resulting device hysteresis loop. Shims were made of steel, aluminium, brass, bisalloy 80, bisalloy 400, and bisalloy 500. Each connection used two M16 Grade 8.8 bolts with a 220mm slot length, and a 3-6mm thick shim. The cap, moving and fixed plates of the SHJ are 20mm thick steel. Bolts were consistently tensioned to 390/400 kN, validated as the proof load, to ensure equal comparisons. Table 2 summarises the shim materials.

Table 2. Details of the different shim materials

	Material	Specification
Shim	Aluminium	5005Gp-Series Aluminium
	Brass	UNS C26000-1/2Hard Temper
	Bisalloy 80	Bisplate 80
	Bisalloy 400	Bisplate 400
	Bisalloy 500	Bisplate 500

Sliding Hinge Joint Anti-Corrosion Coatings

The second set of tests examines anti-corrosion coatings. Five anti-corrosion coatings are tested using a 6mm Bisalloy 500 shim specifically: 1) Sweep blasted; 2) alkyd 70%; 3) alkyd 100%; 4) zinc70%; and 5) zinc 100% coatings are tested. The percentages are the amount of the sliding surface covered. The results are used to quantify the impact on friction and force generated.

Sliding Hinge Joint Corrosion Tests

Finally, the original SHJ connections using Bisalloy 500 shim and each type of corrosion coating are subjected to 24 x 6-hour cycles of soaking in salted water, each followed by 18 hours of drying. The tests were carried out with water of 40-50°C and 36g/L of salt concentration. Devices were then tested to quantify the impact of this corrosive environment.

Sliding Hinge Joint Response Modelling

Figure 4 presents an example experimental hysteresis loop. The goal is to model these loops with a fundamental mechanics elasto-plastic model. The Menegotto-Pinto based model is an effective method of simulating the observed elasto-plastic behaviour of the SHJ connection, where the connection force is a function of input displacement.

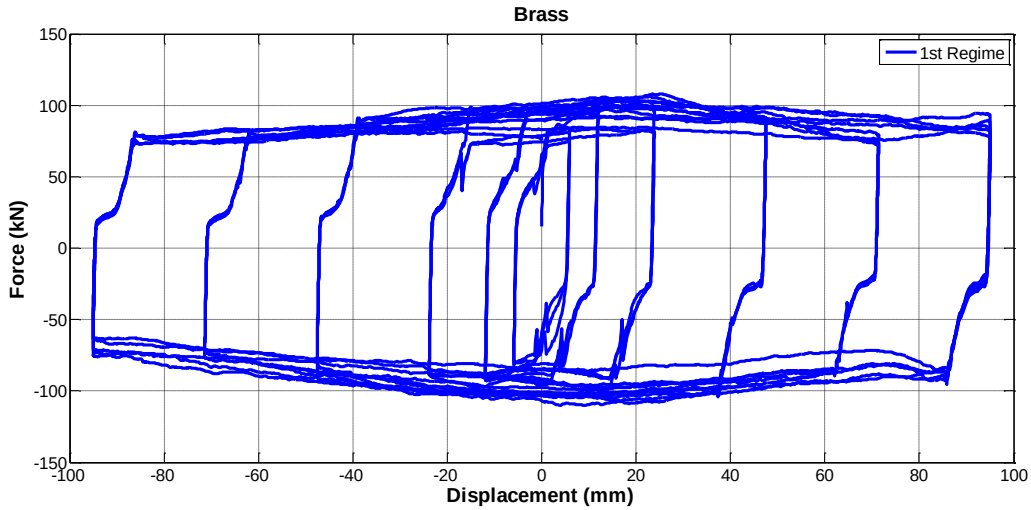

Figure 4. Hysteresis loop for brass shims; Force (kN) over displacement (mm).

Equation (1) presents the fundamental description of the Menegotto-Pinto model:

$$F = \frac{K.(x - x_{reset}) + F_{reset}}{\left(1 + \left|\frac{K.(x - x_{reset}) + F_{reset}}{F_y.(sign(\dot{x}))}\right|^{\beta}\right)^{1/\beta}} \quad (1)$$

Where F_y is the sliding force threshold, K is the initial linear stiffness, x_{reset} is the displacement at the last time the velocity changed sign, F_{reset} is the force at the last time that the velocity changed sign, and β is a constant that determines the rate of divergence. For high values of β the elastic-plastic transition is very sharp, whereas lower values of β give a smoother, more gradual transition. All these terms are defined schematically in Figure 5.

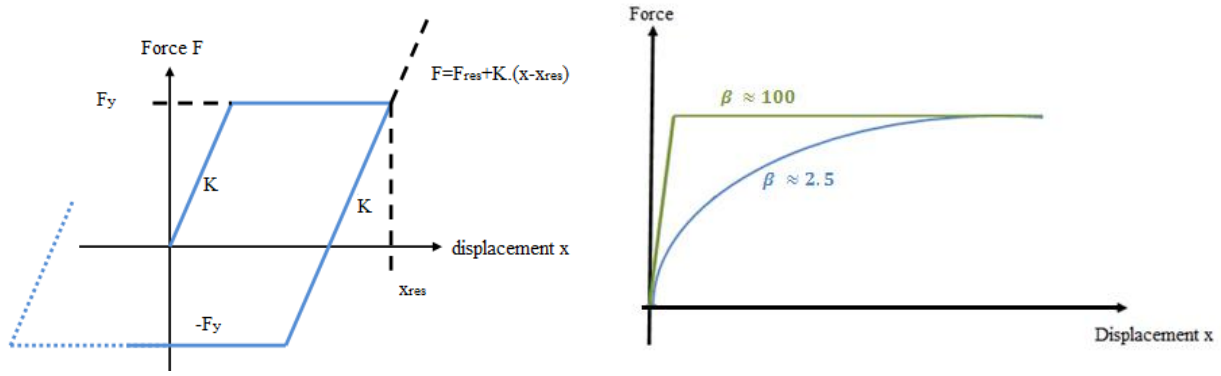

Figure 5. Hysteresis loop parameter definitions the perfect elasto-plastic Menegotto-Pinto model.

Each experiment is modelled and all model parameters identified for each case. A specific added effect included in this work is the addition of velocity dependence, evident in Figure 4, into the Menegotto-Pinto model based on experimental results. This finding is unique to this work as the SHJ was previously considered to be velocity independent (Golondrino et al (2012)). The model including velocity dependence as a linear term is defined:

$$F_{new\ model} = F_{Menegotto\ -Pinto} \cdot (1 + v\ /\ dep) \qquad (2)$$

Where $F_{Menegotto\text{-}Pinto}$ is the force calculated with the Menegotto-Pinto model in Equation (1), v is the velocity, and dep is the velocity dependence factor. The term $(1+v/dep)$ captures the added velocity dependence.

Results and Discussion

Velocity Dependence and Initial Tests

Figure 6 presents the hysteresis loop of a SHJ using brass shims without and with velocity dependence terms. Both panels show experimental and model results. The need for velocity dependence is clear due to the mismatch of the experimental and model results in the top row. The velocity dependence enables the curve of the top and bottom of the loop to be more accurately captured.

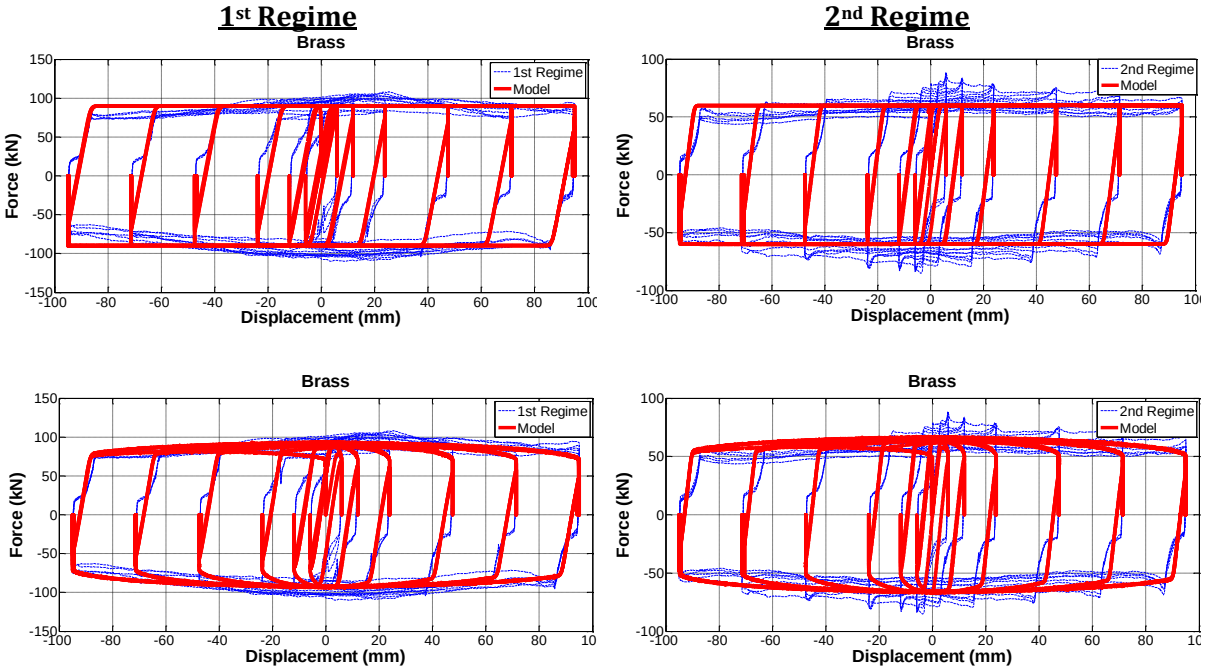

Figure 6. Hysteresis loop for the brass shim. The top row presents model results without velocity dependence, while the bottom row presents model results with velocity dependence.

Table 3 summarises the model parameters for all shim materials and test regimes. The stiffness, the rate of divergence β and the dependence parameter do not change between the 1st and 2nd regime. The only parameter varying is the sliding force F_y, which changes due to degradation of the devices. The quality of fit is similar to those in Figure 6. The velocity dependence is significant and does not change between regimes. It is a unique finding to this work, where previously it was thought that Coulomb friction devices would not display this effect.

Table 3. Model parameters for each shim material

Shim / Tests	Stiffness K (kN.m-1)		Sliding force Fy (kN)		Rate of divergence β		Dep	
	1st Run	2nd Run	1st Run	2nd Run	1st Run	2nd Run	1st Run	2nd Run
Brass	18	18	70	50	100	100	30	30
Aluminium	17.5	17.5	50	45	100	100	60	60
Bisalloy 80	20	20	70	50	100	100	60	60
Bisalloy 400	22	22	65	60	100	100	30	30
Bisalloy 500	18	18	80	70	100	100	60	60

Impacts of Anti-Corrosion Coatings

Figure 7 shows the hysteresis loop of a SHJ with Bisalloy 500 shim with sweep blasted coating. The Menegotto-Pinto model fits the experimental results well. However, a negative velocity dependence parameter was required to match the inverse curve observed. It is clear that this coating acts as a lubricant under a cyclic loading, degrading the level of resistive force. This trend was similar for all but the Alkyd 100 coating, as summarised in Table 4. Table 5 summarises the model parameters for a 2nd set of experimental results on identical connections to those in Table 3, which shows very similar results, as expected. Both tables show a comparison to the uncoated results for Bisalloy 500 in Table 3.

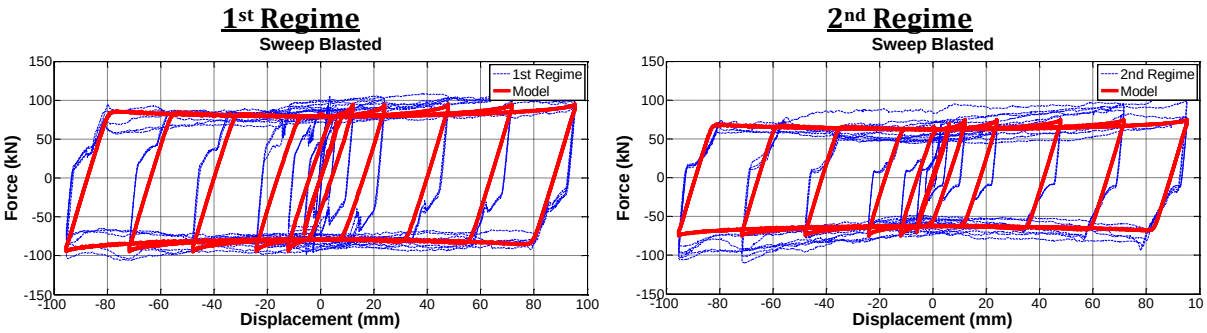

Figure 7. Control coating tests: sweep blasted hysteresis loop.

Table 4. Model parameters for each coating: first set of results.

Control Coating / Tests	K		Fy		B		Dep	
	1st Run	2nd Run	1st Run	2nd Run	1st Run	2nd Run	1st Run	2nd Run
Sweep Blasted	12	12	95	75	10	10	-90	-90
Alkyd 70%	15	15	90	78	10	10	-30	-30
Alkyd 100%	8	8	50	20	10	10	30	30
Zinc 70%	10	10	90	60	10	10	-90	-90
Zinc 100%	10	10	90	60	10	10	-90	-90
Uncoated results Bisalloy 500	18	18	80	70	100	100	60	60

Table 5. Model parameters for each coating: second set of results.

Control Coating / Tests	K		Fy		B		Dep	
	1st Run	2nd Run	1st Run	2nd Run	1st Run	2nd Run	1st Run	2nd Run
Sweep Blasted	14	14	95	75	10	10	-120	-120
Alkyd 70%	15	15	90	78	10	10	-30	-30
Alkyd 100%	12	12	75	45	10	10	-60	-60
Zinc 70%	13	13	90	70	10	10	-60	-60
Zinc 100%	10	10	50	10	10	10	-100	-100
Uncoated results Bisalloy 500	18	18	80	70	100	100	60	60

Impacts of Corrosion

Figure 8 shows the hysteresis loop for a sweep blasted coating after corrosion testing. As previously mentioned, this corrosion testing incorporated 24 x 6-hour cycles of soaking in salted water, each followed by 18 hours of drying. The tests were carried out with water of 40-50°C and 36g/L of salt concentration.

The Menegotto-Pinto fits the experimental results well using a negative velocity dependence parameter. It is similar in shape to Figure 7, for an identical connection, as expected. Table 6-7 summarize the results. Overall, comparing Table 4-5 to Table 6-7, it is clear that the impact of corrosion, as tested, was limited and had no notable effect outside expected variation between devices using the same materials.

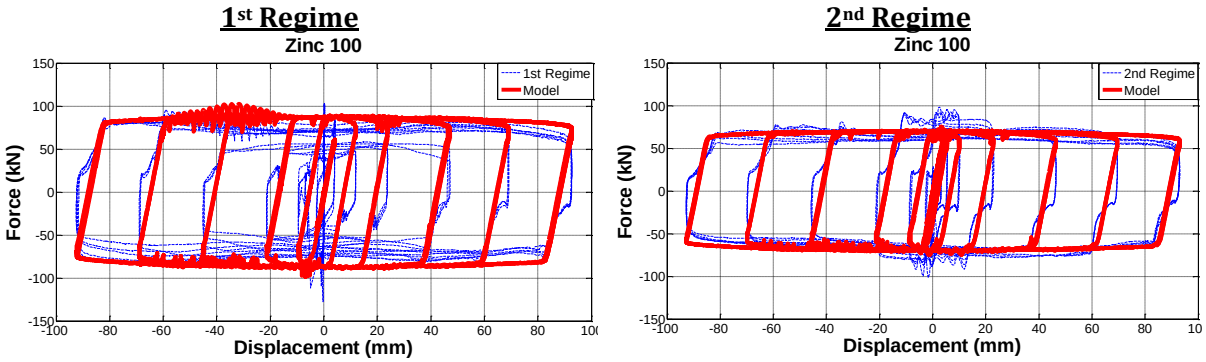

Figure 8. Corrosion tests: sweep blasted Hysteresis Loop.

Table 6. Model parameters for each coating corroded: first set of results

Corrosion / Coating / Tests	K		Fy		B		Dep	
	1st Run	2nd Run	1st Run	2nd Run	1st Run	2nd Run	1st Run	2nd Run
Sweep Blasted	12	12	65	60	10	10	-60	-60
Alkyd 70%	12	12	55	38	10	10	-60	-60
Alkyd 100%	18	18	85	45	10	10	-150	-150
Zinc 70%	18	18	72	65	10	10	90	90
Zinc 100%	15	15	75	60	10	10	90	90

Table 7. Model parameters for each coating corroded: second set of results.

Corrosion / Coating / Tests	K		Fy		B		Dep	
	1st Run	2nd Run	1st Run	2nd Run	1st Run	2nd Run	1st Run	2nd Run
Sweep Blasted	15	15	60	50	10	10	-60	-60
Alkyd 70%	12	12	55	38	10	10	-60	-60
Alkyd 100%	6	6	22	16	10	10	-150	-150
Zinc 70%	18	18	72	65	10	10	-90	-90
Zinc 100%	15	15	75	45	10	10	-90	-90

Overall Results

Figure 9 summarizes the overall results for a Bisalloy 500 shim SHJ. The error bars in Figure 9 show the variation of the results. As shown, the two last values are equal to zero, but it does not mean that no dependence has been found. In fact, the velocity dependence was either positive or negative with the same intensity. Moreover, the bars represent the intensity average of the velocity dependence. The closer the value is to zero, the more important the velocity dependence is. It would therefore be pointless to provide a specific percentage. Only the positive/negative velocity dependence can be noted. Both the coating and corrosion results seem to obtain a negative velocity dependence parameter, except from the non-coated and non-corroded SHJ connection.

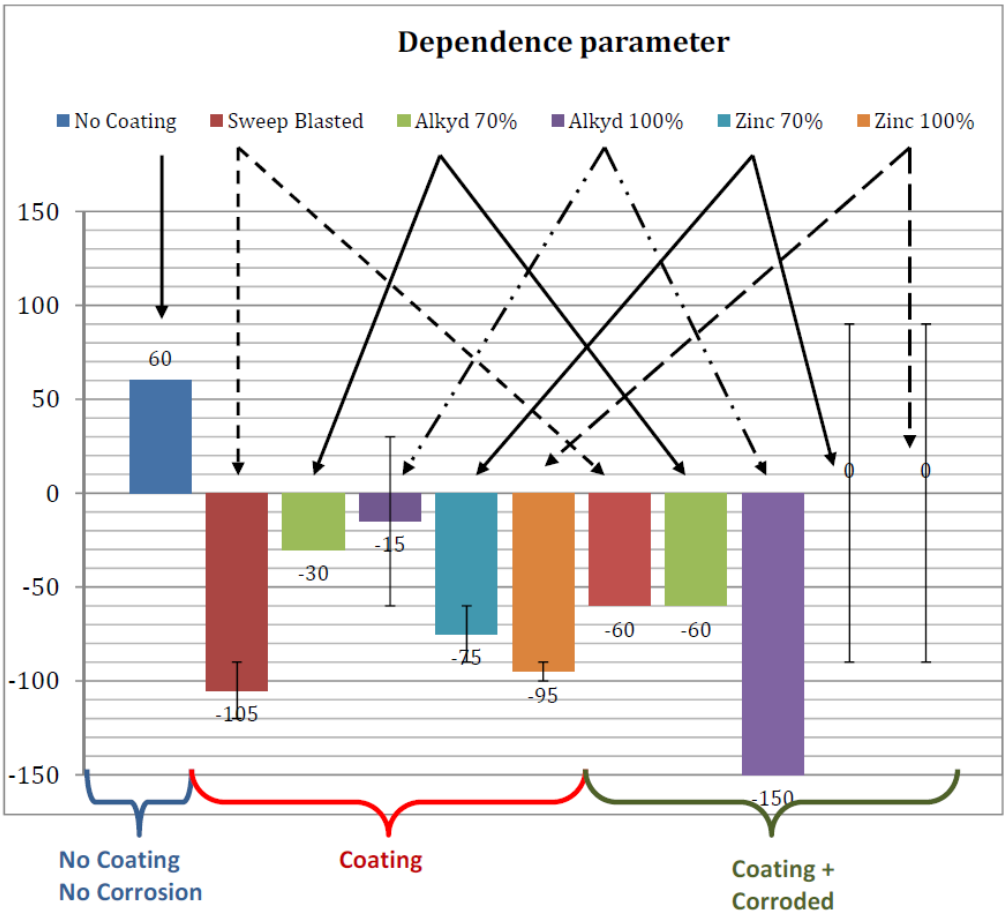

Figure 9. Impact of the corrosion and the corrosion-coating process on the velocity parameter.

Conclusions

This work shows that the Menegotto-Pinto model is a suitable mathematical model for approximating the performance of Sliding Hinge Joints (SHJs). Any device of this type that exhibits consistent behaviour (Hysteresis loop appearing largely rectangular) can be easily simulated with an elasto-plastic Menegotto-Pinto model.

The addition of velocity dependence into the Menegotto-Pinto model improves its ability to replicate experimental results. All experimental results confirm the presence of velocity dependence, which is a novel finding for friction devices, not previously though to exhibit such velocity dependence. At this time, the only conclusions about the dependence are that the anti-corrosion coating process leads to a negative parameter while the sweep blasted non-corroded coating generates a positive parameter and the influence of corrosion on sweep blasted surfaces is minor.

Finally, the results corroborate the idea of low-damaged devices. Degradation of most SHJ connections shows around 20-30% over successive response regimes, which will limit the ability of the SHJ to dissipate energy and limit structural response on successive seismic events. This degradation has also been found by Khoo (Khoo et al, 2012). This degradation must be taken into account be designers, as the SHJ may provide less resistive force during major aftershocks following a primary earthquake.

References

Golondrino, JC, MacRae, GA Chase, JG, Rodgers, GW, and Mora Munoz, A. (2012). “Design Considerations for the Braced Frames with Asymetric Friction Connections,” STESSA 2012 – Behaviour of Steel Structures in Seismic Areas, Santiago, Chile, January 9-12, 8-pages.

MacRae, G.A. (2008), “A New Look at Some Earthquake Engineering Concepts,” Nigel Priestly Symposium, August, King’s Beach, CA.

Clifton, G. C. (2005). "Semi-rigid joints for moment-resisting steel framed seismic-resisting systems," PhD Thesis, The University of Auckland, Auckland, New Zealand.

Clifton GC, MacRae GA, Mackinven H, Pampanin S, Butterworth J.(2007) Sliding Hinge Joints and Subassemblies for Steel Moment Frames, New Zealand Society for Earthquake Engineering Annual Conference, Paper 19, Palmerston North.

Clifton, G. C., Butterworth, J.W., Zaki, R. (2004) 'Two New Semi-Rigid Joints for Moment-Resisting Steel Frames', 7th Pacific Structural Steel Conference, Proceedings 7th Pacific Structural Steel Conference, Long Beach, California, March, 2004, p.1-14

Khoo H.H., Clifton G.C., Butterworth J., MacRae, G.A. (2012) Development of self-centering sliding hinge joint, Proceedings of the 2012 New Zealand Society for Earthquake Engineering (NZSEE) Annual Conference, Christchurch, New Zealand, 13-15 April 2012

Rodgers, G.W., Chase, J.G., Mander, J.B., Leach, N.C. and Denmead, C.S. (2007). “Experimental Development, Tradeoff Analysis and Design Implementation of High Force-To-Volume Damping Technology,” NZSEE Bulletin, Vol 40(2), pp. 35-48, ISSN No. 1174-9857.

Rodgers, GW, Mander, JB, Chase, JG, Leach, NC, and Denmead, CS (2008). “Spectral Analysis and Design Approach for High Force-to-Volume Extrusion Damper-based Structural Energy Dissipation,” Earthquake Engineering & Structural Dynamics (EESD), Vol 37(2), pp. 207-223, ISSN: 0098-8847.